Journal of Alloys and Compounds 502 (2010) 472–476

Contents lists available at ScienceDirect

Journal of Alloys and Compounds

journal homepage: www.elsevier.com/locate/jallcom

Characterization and optimization of $Ln_{1.7}Sr_{0.3}CuO_4$ (Ln = La, Nd)-based cathodes for intermediate temperature solid oxide fuel cells

Xifeng Ding*, Xin Kong, Xiong Wang, Jinguo Jiang, Chong Cui

Department of Materials Science and Engineering, Nanjing University of Science and Technology, Nanjing, Jiangsu 210014, PR China

ARTICLE INFO

Article history:
Received 1 July 2009
Received in revised form 26 April 2010
Accepted 28 April 2010
Available online 5 May 2010

Keywords:
SOFC
Cathode
Ln_2CuO_4
Electrochemical performance

ABSTRACT

The $Ln_{1.7}Sr_{0.3}CuO_4$ (Ln = Nd, La), *i.e.*, NSCu and LSCu materials with perovskite-related structure were synthesized and evaluated as new cathodes for intermediate temperature solid oxide fuel cells (IT-SOFCs). The crystal structure, thermal expansion, electrical conductivity and electrochemical performance of $Ln_{1.7}Sr_{0.3}CuO_4$ cathodes have been investigated by X-ray diffraction, dilatometry, DC four-probe method, AC impedance and cyclic voltammetry (CV) techniques. The conductivity of NSCu and LSCu reached 106 S cm^{-1} and 125 S cm^{-1} at 800 °C. NSCu cathode exhibited much lower area specific resistances (ASR) than LSCu, e.g., the ASR values for NSCu cathode on Sm-doped ceria (SDC) electrolyte in air were 0.07 Ω cm^2, 0.09 Ω cm^2 and 0.24 Ω cm^2 at 800 °C, 750 °C and 700 °C, while the corresponding values for LSCu were 0.11 Ω cm^2, 0.21 Ω cm^2 and 0.44 Ω cm^2, respectively. To further optimize the electrochemical performance of the cathodes, a certain amount of Sm-doped ceria (SDC) electrolyte was introduced. The polarization resistance of NSCu–SDC30 and LSCu–SDC30 was 0.12 Ω cm^2 and 0.18 Ω cm^2 at 700 °C in air, nearly half of pure NSCu and LSCu, respectively.

1. Introduction

Solid oxide fuel cells (SOFCs) have attracted great attention because of their high energy conversion efficiency, environmental compatibility and excellent fuel flexibility. Typical SOFCs operate at high-temperature (~1000 °C), leading to a series of problems such as limited choice of interconnect materials, chemical reactivity between cell components and thermal expansion mismatch [1–3]. Developments of the intermediate temperature solid oxide fuel cells (IT-SOFCs) operating below 800 °C make it possible to use less expensive construction materials, to suppress degradation caused by high operating temperatures, and to improve efficiency of the kW scale generators [4–6].

A major issue with reduced temperature is the decrease of the catalytic activity for oxygen reduction of the cathode [7,8]. The development of new cathode materials with low polarization resistance therefore attracted great interest. Previously, many studies have shown that mixed ionic-electronic conducting (MIEC) materials with K_2NiF_4-type structure exhibited excellent catalytic activity for oxygen reduction. Compared with the commonly used perovskite cathodes, K_2NiF_4-type structure materials possess better thermal stability, lower thermal expansion coefficient and higher oxide-ion diffusivity [9]. Among K_2NiF_4-type compounds for potential use of SOFC cathodes, Ln_2NiO_4 (Ln = La, Pr, Nd or Sm)-based materials have attracted most attention [10–20]. For instance, the $Nd_{1.6}Sr_{0.4}NiO_4$ electrode exhibited a polarization resistance of 0.93 Ω cm^2 at 700 °C and the highest current density of 125 mA cm^{-2} at overpotential of 200 mV [19]. In the investigation of Ln_2NiO_4 (Ln = La, Pr, Nd) compounds [20], Mauvy et al., found that $Nd_2NiO_{4+\delta}$ was in particular promising due to its low reactivity with YSZ and high electrochemical activity obtained under polarization. However, layered cuprate compositions (Ln_2CuO_4), previously received fairly intensive attention with respect to their superior electrical properties at low temperatures [21], have been less evaluated as cathode materials for SOFCs [22,23]. Li et al. [22] investigated $La_{2-x}Sr_xCuO_{4-\delta}$ (x = 0, 0.1, 0.3, 0.5) series oxides as prospective cathode for IT-SOFCs based on ceria electrolytes, and $La_{1.7}Sr_{0.3}CuO_{4-\delta}$ electrode exhibited the lowest overpotential about 100 mV at a current density of 150 mA cm^{-2} at 700 °C in air among $La_{2-x}Sr_xCuO_{4-\delta}$ materials.

Up to now, the researches based on Ln_2CuO_4 type oxides as cathode materials are mainly focused on La at Ln-site. Little attention has been paid to other rare earths. In this study, $Ln_{1.7}Sr_{0.3}CuO_4$ (Ln = Nd, La) compounds were evaluated as potential cathode materials for IT-SOFCs. The phase structure, thermal expansion property and electrochemical property were investigated. Moreover, in order to further increase the electrocatalytic activity for oxygen reaction, Sm-doped ceria (SDC) electrolyte was introduced into Ln_2CuO_4, and the AC impedance spectroscopy and polarization characteristics of Ln_2CuO_4–SDC composite cathode were further investigated.

* Corresponding author. Tel.: +86 25 84313329.
E-mail address: dingxifeng2002@163.com (X. Ding).

0925-8388/$ – see front matter © 2010 Elsevier B.V. All rights reserved.
doi:10.1016/j.jallcom.2010.04.199

2. Experimental

2.1. Synthesis of $Ln_{1.7}Sr_{0.3}CuO_4$ powder

The $Nd_{1.7}Sr_{0.3}CuO_4$ (NSCu) and $La_{1.7}Sr_{0.3}CuO_4$ (LSCu) powders were synthesized via a combined EDTA–citrate complexing sol–gel method. EDTA (0.04 mol) was dissolved in 1 M $NH_3{\cdot}H_2O$ solution to prepare $NH_3{\cdot}H_2O$–EDTA buffer solution. Nd_2O_3 and La_2O_3 powders were separately dissolved in diluted nitric acid with heating and magnetic stirring before applying the sol–gel synthesis. Then, the calculated amount of metal nitrates $Sr(NO_3)_2$, $Cu(NO_3)_3{\cdot}3H_2O$ was prepared separately as an aqueous solution and then dissolved in the above EDTA–$NH_3{\cdot}H_2O$ solution under heating and stirring. After stirring for certain time, a certain amount of citric acid was added. The mole ratio of EDTA, citric acid and total metal ions was controlled around 1:1.05:1. $NH_3{\cdot}H_2O$ was then added to adjust pH values to ~6 to avoid the precipitation occurrence after citric acid addition. The solution was kept stirring and heating at 80 °C. With the evaporation of water, a dark purple gel was obtained. The gelled samples were baked in a drying oven at 120 °C. Finally, the dried gel was calcined twice at 950 °C for 2 h in air. The as-synthesized powders were ball-milled by zirconia balls for 30 min to break up any agglomerations which were formed during the calcination.

2.2. Preparation of cathode

Symmetrical electrochemical cells consisting of porous electrodes and dense SDC electrolyte were fabricated to test the electrochemical characteristics. Uniaxially pressed SDC electrolyte disks were sintered at 1550 °C for 2 h in air with the resulting dimension about 12 mm in diameter and 1 mm in thickness. The electrode pastes were prepared by mixing the calcined LnSCu powder with ethylcellulose at a weight ratio of 10:1, and then mixed with terpineol as a solvent. Then, the LnSCu pastes with an area of 0.25 cm^2 were screen-printed on both sides of SDC disks and then calcined at 950 °C for 2 h in air. Silver paste was brushed onto the SDC disk about 4 mm away from LnSCu electrodes with a ring shape, and sintered at 700 °C for 30 min. The Pt grids and leads were stuck with Ag current collector for the electrochemical property measurements.

2.3. Characterization

The decomposition and crystallization behaviors of the polymetric precursor were analyzed by thermogravimetry-differential analysis (TG/DSC, STA449C, NETZSCH) at a heating rate of 10 °C min^{-1} up to 1000 °C. The phase identification of the synthesized powders was performed by X-ray diffraction with an ARL X-ray powder diffractometer using Cu Kα radiation. For electrical conductivity and thermal expansion measurements, the as-synthesized powders were granulated with 5 wt.% PVA and pressed into rectangular bars with nominal dimensions of 64 mm × 5 mm × 5 mm under 50 MPa. Then the bars were sintered at 1200 °C for 2 h. The electrical conductivity of sintered rectangular bars was measured in open air from 300 °C to 800 °C using DC four-terminal method. The thermal expansion of the rectangular specimens was measured from room temperature to 800 °C in air, using a dilatometer (RPZ-01, Luoyang, China) with a heating rate of 5 K/min. Electrochemical impedance spectroscopy (EIS) measurements of the electrode materials on the SDC electrolyte were carried out with excitation potentials of 10 mV over a frequency range from 100 KHz to 0.1 Hz generated by an impedance analyzer (CHI 660C electrochemical workstation, Chenhua, China) in the temperature range from 500 °C to 800 °C. Cyclic voltammetry (CV) measurements (5 mV/S) were performed using CHI 660C. The IR drop originating from the electrolyte resistance as compensated by a postfactum correction of the CVs, using the series resistance obtained from the EIS data, in order to establish the resistance-free *i–E* characteristics.

3. Results and discussion

3.1. TG and DTA analysis

Fig. 1 is the TG/DSC results of the dried $La_{1.7}Sr_{0.3}CuO_4$ (LSCu) polymeric resin, and the corresponding curves of $Nd_{1.7}Sr_{0.3}CuO_4$ (NSCu) are very similar with LSCu. From 100 °C up to about 210 °C, the mass has a slow decrease with increasing temperature, which could be ascribed to the volatilization of water. And then, the mass has a sharp decrease with a weight loss about 80% until 600 °C, together with a strong and sharp exothermic peak presented in the DSC pattern around 460 °C. Such an exothermic effect is associated with the decomposition and oxidation of the metal-chelates, and reactions of the decomposed chelates [24]. Followed by the decomposing reaction of metal-chelates, the crystallization of perovskite-related oxide occurs. At a temperature higher than 700 °C, the mass weight then keeps almost constant, indicating that the decomposition reaction and phase formation have completed.

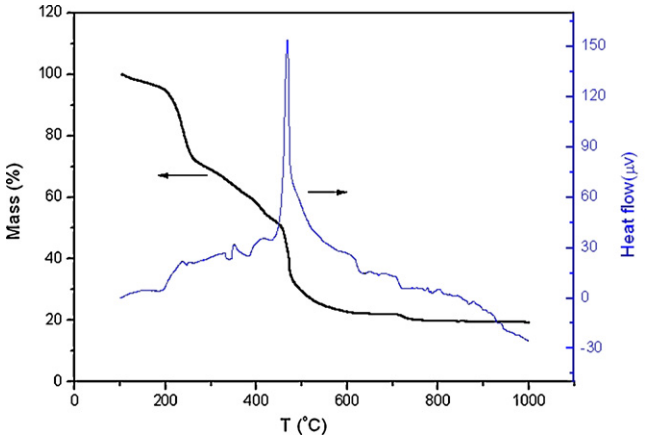

Fig. 1. TG-DTA curves for $La_{1.7}Sr_{0.32}CuO_4$ (LSCu) dried polymeric resin.

3.2. XRD analysis

Fig. 2 presents XRD pattern of NSCu and LSCu powders after calcination at 950 °C for 2 h in air. The prepared $Ln_{1.7}Sr_{0.3}CuO_4$ (Ln = La, Nd) compositions are found as single phase. All the peaks can be well indexed as K_2NiF_4 tetragonal structure with the space group of *I*4/*mmm*. The lattice parameters of NSCu and LSCu are calculated to be $a = 0.3942(5)$ nm $c = 1.213(4)$ nm and $a = 0.3778(5)$ nm and $c = 1.318(7)$ nm, respectively, using software Jade 5 after cell refinement [25]. The crystal lattices of the Nd-containing compounds are about 0.63% more compact in comparison with the corresponding La-contained copper oxides. This correlates with the smaller ionic radii of Nd^{3+} (0.100 nm) than La^{3+} (0.106 nm).

3.3. Electrical conductivity

For perovskite-related MIEC electrode material, the co-existence of electronic holes and oxygen vacancies makes them simultaneously possess both electronic and ionic conductivities. As the electronic conductivity is commonly at least one order higher than ionic conductivity for cathode materials, the measured total conductivity values can be mainly referred to electronic conductivity. The total electrical conductivity as a function of temperature measured by the four-terminal method is shown in Fig. 3. It can be found that LSCu and NSCu exhibit different conducting behaviors

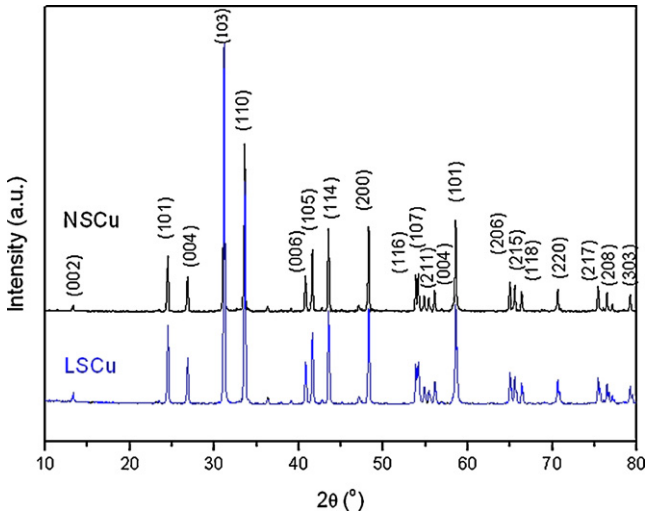

Fig. 2. XRD patterns of $La_{1.7}Sr_{0.3}CuO_4$ (LSCu) and $Nd_{1.7}Sr_{0.3}CuO_4$ (NSCu) powders calcined at 950 °C for 2 h.

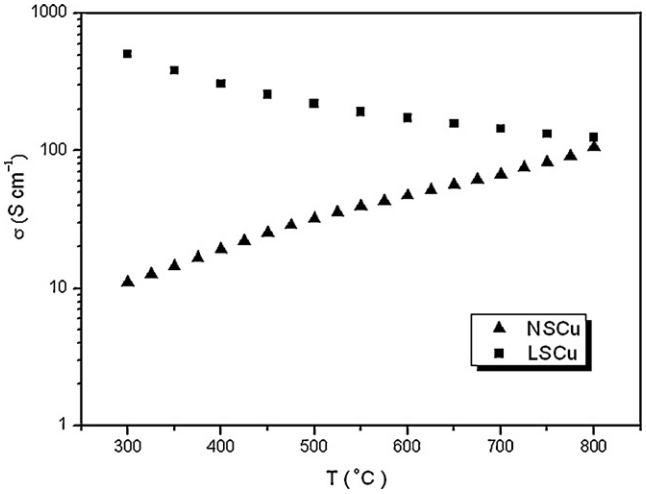

Fig. 3. The electrical conductivity of NSCu and LSCu specimens as a function of temperature.

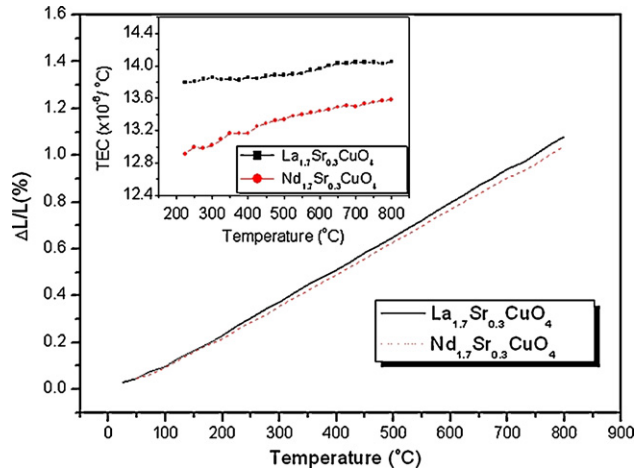

Fig. 4. Thermal expansion coefficients of $La_{1.7}Sr_{0.3}CuO_4$ and $Nd_{1.7}Sr_{0.3}CuO_4$ specimens on the temperature range 200–800 °C.

with temperature, *i.e.*, the conductivity of LSCu decreases with increasing temperature, implying a metallic behavior, but increases with the elevated temperature for NSCu, as typical for semiconductor. The conductivity of NSCu and LSCu reaches 106 S cm^{-1} and 125 S cm^{-1} at 800 °C, indicating they are excellent conductors to be used as electrodes for SOFCs.

3.4. Thermal expansion of LSCu and NSCu

The thermal expansion behaviors of $La_{1.7}Sr_{0.3}CuO_4$ and $Nd_{1.7}Sr_{0.3}CuO_4$ in air are shown in Fig. 4. The thermal expansion coefficients (TECs) of LSCu are larger than those of NSCu. For instance, the TEC from room temperature to 600 °C is 14.0×10^{-6}/°C for LSCu, while the corresponding value is 13.5×10^{-6}/°C for NSCu. It seems that TEC values of $Ln_{1.7}Sr_{0.3}CuO_4$ are proportional to the radii of rare earth ions. A similar trend has also been observed for

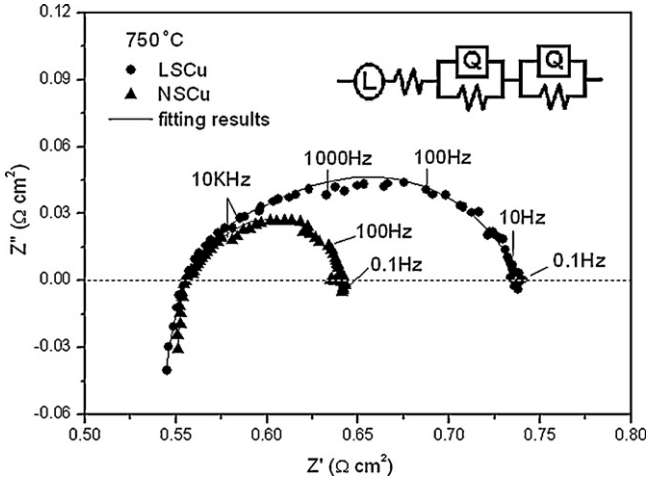

Fig. 5. Electrochemical impedance spectroscopy for $Nd_{1.7}Sr_{0.3}CuO_4$ (LSCu) and $La_{1.7}Sr_{0.3}CuO_4$ (NSCu) cathodes on SDC electrolyte at 750 °C under open circuit potential in air. *Insert*: The equivalent circuit of the impedance for the above cathodes.

other perovskite systems, such as $Ln_{0.6}Sr_{0.4}CoO_{3-\delta}$ (Ln = La, Pr, Nd, Sm, Gd) [26] and $Ln_{1-x}Sr_xMnO_3$ (Ln = Pr, Nd, Sm and Gd) [27]. In general, the compound with ionic bond has a larger thermal expansion than that with covalent bond [26]. The percent ionic character of a bond is related to the electronegativity difference between the bonded atoms *A* and *O* in the *A*–*O* bond by the following relationship [26]:

$$\%\ \text{ionic character} = \{1 - \exp[-0.25(x_A - x_O)^2]\} \times 100 \quad (1)$$

where x_A and x_o are the electronegativities of the *A* and *O* atom (x_o = 3.44), respectively. Since the Pauling electronegativity of La (x_{La} = 1.10) is smaller than Nd (x_{Nd} = 1.14) atom, it can be concluded that the decreased ionic character of Nd–O bond results in a lower TEC for NSCu. The lower TEC can improve the thermal expansion compatibility between the cathode and electrolyte, which may further reduce the cathodic interfacial polarization resistances.

3.5. EIS of LSCu and NSCu

AC impedance studies were carried out using NSCu and LSCu cathodes deposited on SDC electrolyte based on a symmetrical cell configuration in air. The Nyquist plots for NSCu and LSCu at 750 °C are shown in Fig. 5. The data were fitted by a nonlinear least square fitting program (ZSimpWin 3.21) and the equivalent circuit with a configuration of $LR_s(R_1Q_1)(R_2Q_2)$ is exhibited in inset of Fig. 5, where R_s is primarily the electrolyte ohmic resistance (the electrode ohmic resistance and the contact resistance are negligibly small), *L* is the inductance, which would be ascribed to the Pt current/voltage probes or the instrument, R_1 and R_2 are the electrode polarization resistances at high and low frequency, Q_1 and Q_2 are the corresponding constant phase elements. The results of this study are generally in agreement with the previous workers [26–28] that the arc at high frequency is related to the polarization during the migration of the oxygen ions, and the arc at low frequency may be attributed to the electrode polarization caused by the adsorption/desorption of the molecular oxygen. The fitting

Table 1
Parameters obtained from the data fitting to the equivalent circuit shown in Fig. 5 of NSCu and LSCu cathodes on SDC electrolyte at 750 °C.

Cathode	R_s (Ω cm^2)	R_1 (Ω cm^2)	n_1	Q_1 (Ω cm^{-2})	R_2 (Ω cm^{-2})	Q_2 (Ω cm^2)	n_2	R_p[a] (Ω cm^2)
NSCu	0.548	0.021	0.609	0.002	0.072	0.004	0.797	0.093
LSCu	0.541	0.102	0.474	0.003	0.115	0.004	0.697	0.217

[a] R_p is the total polarization resistance including R_1 and R_2, *i.e.*, $R_p = R_1 + R_2$.

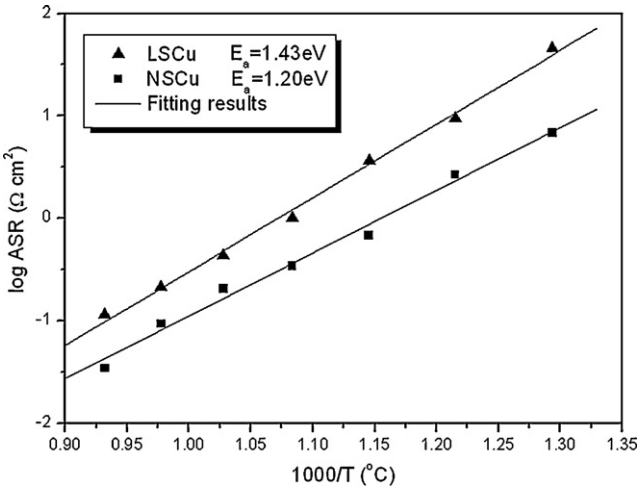

Fig. 6. Temperature dependence of R_p for LSCu and NSCu in air.

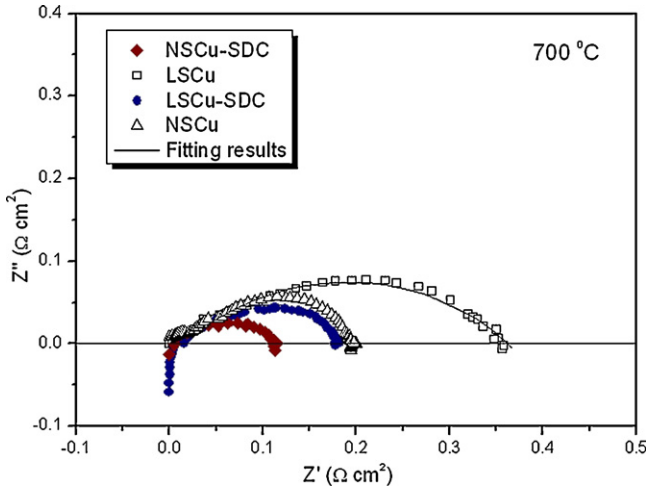

Fig. 7. Electrochemical impedance spectroscopy for NSCu–SDC, LSCu–SDC composite cathodes and NSCu, LSCu pure cathodes on SDC electrolyte at 750 °C under open circuit potential in air.

results are shown in Table 1. It can be found that R_2 values for both cathodes are much higher than R_1, indicating that total reaction rate determining step is the diffuse process. Moreover, these parameters are also related to the capacitance and angular relaxation frequency. The capacitance can be calculated according to [11]:

$$C = \frac{(RQ)^{1/n}}{R} \quad (2)$$

The values of capacitance related to high frequency are calculated to be 42 μF cm^{-2} and 31 μF cm^{-2} for NSCu and LSCu cathodes, respectively, which is very close to the reported capacitance value of 42 μF cm^{-2} for the ion-transfer processes of BSCF [7], indicating that the arc at high frequency is related to the polarization during the migration of the oxygen ions. The capacitance values related to low frequency are 0.49 mF cm^{-2} and 0.12 mF cm^{-2}, which is involved in adsorption/desorption process [11]. The total polarization R_p (the sum of R_1 and R_2) of NSCu cathode is 0.093 Ω cm^2, about half of LSCu at 750 °C. Fig. 6 demonstrates R_p values of NSCu and LSCu from 500 °C to 800 °C in an Arrhenius plot. The NSCu cathode shows lower polarization resistance for oxygen reduction, which could be attributed to its lower activation energy for ionic transfer and better thermal expansion compatibility with SDC electrolyte, making this mixed conducting material a promising cathode for intermediate temperature SOFCs.

It has been reported in numerous papers [29–33] that a composite cathode is usually beneficial for further lowering the interfacial polarization resistance of MIEC cathodes. Hence, the NSCu–SDC composite cathode consisting of 70 wt.%NSCu + 30 wt.%SDC has been fabricated and is expected to further increase the electrochemical performance. For comparison, LSCu–SDC with the same weight ratio is also investigated.

3.6. EIS of NSCu–SDC and LSCu–SDC

Fig. 7 shows the EIS of NSCu–SDC and LSCu–SDC composite cathodes at 700 °C in air. For comparison, the EIS of NSCu and LSCu cathodes are also presented. It is worthy of noting that the polarization resistances (simply seen as the low frequency intercept at Z' axis) of composite cathodes are much lower than pure NSCu and LSCu. The polarization resistance of NSCu–SDC and LSCu–SDC is 0.12 Ω cm^2 and 0.18 Ω cm^2 at 700 °C in air, nearly half of NSCu and LSCu, respectively. The decreased resistance of composite cathode is mainly attributed to the reduction of the interfacial resistance between LnSCu cathode and SDC electrolyte [34]. As reported, the LnSCu with K_2NiF_4-type structure is one kind of mixed ionic-electronic conductor, the oxygen reduction reaction occurs not only at the triple phase boundary (TPB) but also on the surface of cathode. The adsorbed molecular oxygen is reduced to oxygen ions, and then diffuse to the electrode–electrolyte interface, and finally to electrolyte bulk. The diffusion rate is affected by the concentration of oxygen vacancies [29]. The addition of the ionic conducting phase (SDC) enhanced the oxygen ionic conductivity, *i.e.*, the concentration of total oxygen vacancies, and thus reduced the resistance. Furthermore, the thermal expansion mismatch between the electrode and electrolyte was also decreased by the composite electrode, and the adhesion of the electrode to the electrolyte was improved.

3.7. Polarization characteristics of NSCu–SDC and LSCu–SDC

Fig. 8a illustrates the IR-compensated current density *vs.* overpotential (i/η) relationship of the oxygen reduction reaction (ORR) at NSCu–SDC and LSCu–SDC cathodes at 700 °C in air. All i/η curves shown in this paper are corrected for the *IR* drop between the working electrode (WE) and reference electrode (RE), using R_s obtained from the EIS measurements, and all current densities refer to the geometric area. It is observed that the cathode overpotential of NSCu–SDC is lower than LSCu–SDC at the same current density. This result is in accordance with EIS data shown in Fig. 7. When the cathodic overpotential is about 0.07 V at 700 °C in air, the current density reaches 0.49 A cm^{-2} for NSCu–SDC.

At low overpotential (within ±34 mV at 700 °C [35]), the current density *vs.* overpotential appears to be a linear relationship:

$$i = i_0 \frac{nF}{RT\upsilon}\eta \quad (3)$$

where i_0 is the exchange-current density, F is the Faraday constant, R is the gas constant and T is the absolute temperature. For the ORR, n and υ are assumed to be 4 and 1, respectively (as the total number of electrons passed per molecule of oxygen reduction is 4 and the rate limiting step would likely have a stoichiometry of 1 for the oxygen reduction reaction) [28]. The least square fitting was performed in the range of −20 to 0 mV of the cathodic overpotential and the fitting results were in good agreement with the measured data (Fig. 8b). The polarization resistance of NSCu–SDC composite cathode, calculated from the derivative of η/i in Fig. 8b, is 0.14 Ω cm^2 at 700 °C, which is very close to the result obtained from aforementioned EIS measurement (0.12 Ω cm^2).

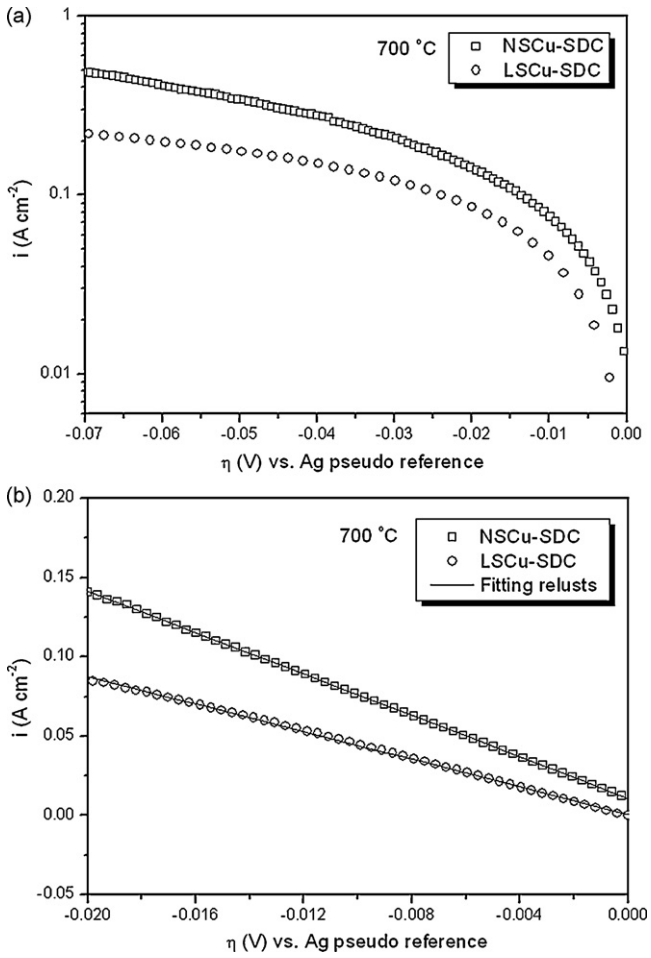

Fig. 8. IR-compensated *i*/*E* relationship (5 mV/s) of O_2 reduction at NSCu–SDC and LSCu–SDC composite cathodes on SDC electrolyte at 700 °C in air (a: Tafel curves and b: linear fitting results in the low-field cathodic overpotential).

4. Conclusions

The $Ln_{1.7}Sr_{0.3}CuO_4$ (Ln = Nd, La) powders with K_2NiF_4-type perovskite-related structure were prepared by EDTA–citrate complexing method and characterized. The conductivities of NSCu and LSCu reach106 S cm^{-1} and 125 S cm^{-1} at 800 °C, indicating they are excellent conductor to be used as electrode for SOFCs. The thermal expansion coefficients of NSCu are lower than those of LSCu, which could be ascribed to the decreased ionic character of Nd–O bond. The total polarization resistances of NSCu cathode are 0.093 Ω cm^2, which is about half of LSCu at 750 °C. The composite cathode was adopted to further lower the interfacial polarization resistance of these MIEC cathodes. The LnSCu–SDC (Ln = La, Nd) composite cathodes consisting of 70 wt.%LnSCu + 30 wt.%SDC (abbreviated as LSCu–SDC and NSCu–SDC) have been investigated. The polarization resistance of NSCu–SDC and LSCu–SDC is 0.12 Ω cm^2 and 0.18 Ω cm^2 at 700 °C in air, nearly half of NSCu and LSCu, respectively. This is attributed to the improvement of the oxygen vacancies concentration and the thermal expansion compatibility after the addition of the ionic conducting phase (SDC). The higher catalytic activity for oxygen reduction makes NSCu–SDC a promising cathode for intermediate temperature SOFCs based on doped ceria electrolytes.

Acknowledgements

The authors gratefully acknowledge the research fundings provided by the Natural Science Foundation of China (No. 50902069), Postdoctoral Science Foundation of China (No. 20070421010), Postdoctoral Science Foundation of Jiangsu Province (No. 0702043C) and Science and Technology Development Foundation of Nanjing University of Science and Technology (No. AB96356).

References

[1] B.C.H. Steel, A. Heinzel, Nature 414 (2001) 345–352.
[2] Z. Shao, S.M. Haile, Nature 431 (9) (2004) 170–173.
[3] X.Z. Zhang, B. Lin, Y.H. Ling, Y.C. Dong, G.Y. Meng, X.Q. Liu, J. Alloys Compd. (2010), doi:10.1016/j.jallcom.2010.03.084.
[4] W.X. Zhu, Z. Lü, S.Y. Li, B. Wei, J.P. Miao, X.Q. Huang, K.F. Chen, N. Ai, W.H. Su, J. Alloys Compd. 465 (2008) 274–279.
[5] X.F. Ding, C. Cui, X.J. Du, L.C. Guo, J. Alloys Compd. 488 (2009) 418–421.
[6] H.P. Ding, X.J. Xue, J. Alloys Compd. 496 (2010) 683–686.
[7] F.S. Baumann, J. Fleig, H.-U. Habermeier, J. Maier, Solid State Ionics 177 (2006) 3187–3191.
[8] K.T. Lee, A. Manthiram, J. Electrochem. Soc. 152 (1) (2005) A197–A204.
[9] S.J. Skinner, J.A. Kilner, Solid State Ionics 135 (2000) 709–712.
[10] J. Wan, J.B. Goodenough, J.H. Zhu, Solid State Ionics 178 (2007) 281–286.
[11] M.J. Escudero, A. Aguadero, J.A. Alonso, L. Daza, J. Electroanal. Chem. 611 (2007) 107–116.
[12] M.L. Fontaine, C. Laberty-Robert, F. Ansart, P. Tailhades, J. Power Sources 156 (2006) 33–38.
[13] A. Aguadero, J.A. Alonso, M.T. Fernández-Díaz, M.J. Escudero, L. Daza, J. Power Sources 169 (2007) 17–24.
[14] C. Lalanne, F. Mauvy, E. Siebert, M.L. Fontaine, J.M. Bassat, F. Ansart, P. Stevens, J.C. Grenier, J. Eur. Ceram. Soc. 27 (2007) 4195–4198.
[15] H. Zhao, F. Mauvy, C. Lalanne, J.-M. Bassat, S. Fourcade, J.-C. Grenier, Solid State Ionics 179 (2008) 2000–2005.
[16] Y. Cao, H.T. Gu, H. Chen, Y.F. Zheng, M. Zhou, C. Guo, Int. J. Hydrogen Energy (2010), doi:10.1016/j.ijhydene.2010.03.046.
[17] A.V. Kovalevsky, V.V. Kharton, A.A. Yaremchenko, Y.V. Pivak, E.N. Naumovich, J.R. Frade, J. Eur. Ceram. Soc. 27 (2007) 4269–4272.
[18] C. Jin, J. Liu, J. Alloys Compd. 474 (2009) 573–577.
[19] L.P. Sun, Q. Li, H. Zhaoa, L.H. Huo, J.C. Grenier, J. Power Sources 183 (2008) 43–48.
[20] F. Mauvy, C. Lalanne, J.M. Bassat, J.C. Grenier, H. Zhao, P. Dordor, Ph. Stevens, J. Eur. Ceram. Soc. 25 (2005) 2669–2672.
[21] J.B. Goodenough, A. Manthiram, J. Solid State Chem. 88 (1990) 115–139.
[22] Q. Li, H. Zhao, L.H. Huo, L. Sun, X.L. Cheng, J.C. Grenier, Electrochem. Commun. 9 (2007) 1508–1512.
[23] M. Soorie, S.J. Skinner, Solid State Ionics 177 (2006) 2081–2086.
[24] X.F. Ding, Y.J. Liu, L. Gao, L.C. Guo, J. Alloys Compd. 458 (2008) 346–350.
[25] J. Chen, F. Liang, L. Liu, S.P. Jiang, L. Jian, Int. J. Hydrogen Energy 34 (6) (2009) 6845–6851.
[26] K.T. Lee, A. Manthiram, J. Electrochem. Soc. 153 (4) (2006) A794–A798.
[27] Y. Sakaki, Y. Takeda, A. Kato, N. Imanishi, O. Yamamoto, M. Hattori, M. Iio, Y. Esaki, Solid State Ionics 118 (1999) 187–194.
[28] J.B. Liu, A.C. Co, S. Paulson, V.I. Birss, Solid State Ionics 177 (2006) 377–387.
[29] T. Horita, K. Yamaji, N. Sakai, H. Yokokawa, A. Weber, E. Ivers-Tiffée, Electrochim. Acta 46 (2001) 1837–1845.
[30] Q.L. Liu, K.A. Khor, S.H. Chan, J. Power Sources 161 (2006) 123–128.
[31] L. Xiong, S.R. Wang, Y.S. Wang, T.L. Wen, J. Alloys Compd. 453 (2008) 356–360.
[32] W.M. Guo, J. Liu, C. Jin, H.B. Gao, Y.H. Zhang, J. Alloys Compd. 473 (2009) 43–47.
[33] X.F. Ding, C. Cui, L.C. Guo, J. Alloys Compd. 481 (2009) 845–850.
[34] C. Jin, J. Liu, J. Alloys Compd. 473 (2009) 573–577.
[35] A.C. Co, S.J. Xia, V. Birss, J. Electrochem. Soc. 152 (3) (2005) A570–A576.